

A Miniature Real-Time Volumetric Ultrasound Imaging System

Ira O. Wygant^a, David T. Yeh^a, Xuefeng Zhuang^a, Amin Nikoozadeh^a, Omer Oralkan^a,
A. Sanli Ergun^a, Mustafa Karaman^b, Butrus T. Khuri-Yakub^a

^aE. L. Ginzton Laboratory, Stanford University, Stanford, CA, USA 94305

^bDepartment of Electronics Engineering, Işık University, Istanbul, Turkey 34398

ABSTRACT

Progress made in the development of a miniature real-time volumetric ultrasound imaging system is presented. This system is targeted for use in a 5-mm endoscopic channel and will provide real-time, 30-mm deep, volumetric images. It is being developed as a clinically useful device, to demonstrate a means of integrating the front-end electronics with the transducer array, and to demonstrate the advantages of the capacitive micromachined ultrasonic transducer (CMUT) technology for medical imaging. Presented here is the progress made towards the initial implementation of this system, which is based on a two-dimensional, 16x16 CMUT array. Each CMUT element is 250 μm by 250 μm and has a 5-MHz center frequency. The elements are connected to bond pads on the back side of the array with 400- μm long through-wafer interconnects. The transducer array is flip-chip bonded to a custom-designed integrated circuit that comprises the front-end electronics. The result is that each transducer element is connected to a dedicated pulser and low-noise preamplifier. The pulser generates 25-V, 100-ns wide, unipolar pulses. The preamplifier has an approximate transimpedance gain of 500 k Ω and 3-dB bandwidth of 10 MHz. In the first implementation of the system, one element at a time can be selected for transmit and receive and thus synthetic aperture images can be generated. In future implementations, 16 channels will be active at a given time. These channels will connect to an FPGA-based data acquisition system for real-time image reconstruction.

Keywords: Capacitive Micromachined Ultrasonic Transducer, CMUT, Two-Dimensional Array, Electronics, Ultrasonic Imaging, Integration, Synthetic Aperture, Flip-Chip Bonding, Through-Wafer Interconnects, Systems

I. INTRODUCTION

A real-time volumetric ultrasound imaging system for a 5-mm endoscopic channel is being developed. The final implementation will provide real-time volumetric images within a 90° by 90° field of view. The system is based on a 16 element by 16 element array of 5-MHz center frequency capacitive micromachined ultrasonic transducers (CMUTs). For improved signal-to-noise ratio (SNR) and to reduce the number of cables connecting the transducer probe to an external system, the transducer array is flip-chip bonded to a custom-designed integrated circuit (IC) that comprises the front-end electronics. The front-end IC is connected to an FPGA-based data acquisition system for real-time image reconstruction. A diagram of the final design is shown in Figure 1.

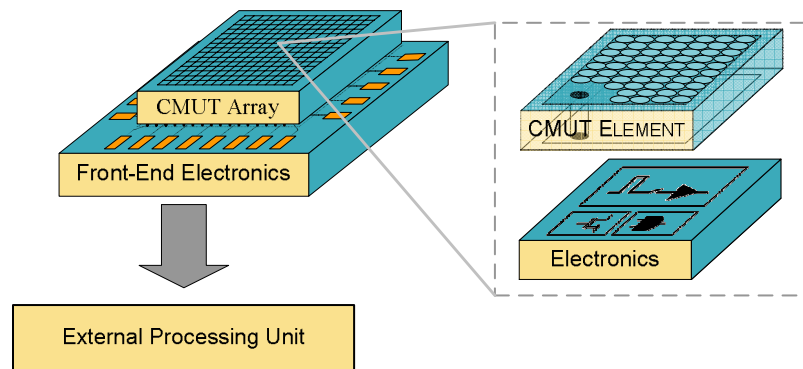


Figure 1: Final system design for a miniature real-time imaging system.

The system is being developed with collaborators in the Stanford Medical School to be a clinically useful device and to demonstrate the advantages of the capacitive micromachined ultrasonic transducer (CMUT) technology for medical imaging. Currently available ultrasound imaging systems designed for use with a catheter or endoscope are limited by the packaging requirements and the piezoelectric transducer technology. The packaging is difficult because the imaging probe must fit inside a small channel, typically several millimeters in diameter. Using piezoelectric materials, it is difficult to make two-dimensional arrays small enough for these channels. Furthermore, the imaging probe must be connected to an external unit with lengthy cables that can present significant parasitic capacitance. To avoid the deleterious effects of the cables, a preamplifier can be integrated with the transducer. If some type of multiplexing is also included in the front-end circuitry, then the number of cables connecting the probe to an external system can be reduced. In this system, through-wafer interconnects [1,2,3] and flip-chip bonding are used to connect the transducer array to the front-end electronics. The through-wafer interconnects occupy little space compared to the active elements and thus efficient connections can be made to large two-dimensional arrays. Furthermore, flip-chip bonding is a proven and reliable technology that provides low impedance connections. It is commonly used in industry to make hundreds of connections between integrated circuits.

The CMUT technology is crucial to the realization of this system. Existing imaging systems for use with a catheter or endoscope are based on piezoelectric transducers. The methods used to fabricate piezoelectric transducers make it difficult to reliably fabricate two-dimensional arrays small enough for use inside a catheter or endoscope. The fabrication is even more difficult for high-frequency transducer arrays. Due to the surface and bulk micromachining methods used to fabricate CMUTs, CMUT arrays of arbitrary size and shape, and with elements with center frequencies greater than 40 MHz can be fabricated as easily as traditional one-dimensional arrays. Silicon bulk micromachining is used in this system to create the through-wafer interconnects. In summary, the resolution of an imaging system based on the CMUT is improved due to the CMUT's larger bandwidth, increased flexibility in array design, and the option to use higher frequencies.

This paper presents the progress we've made in the development of the system shown in Figure 1. Initially, we are building a simpler system that differs from the final system in that the element size is 250 μm by 250 μm , a single element at a time is selected for transmit and receive, and image reconstruction is done offline. Results from fabricated two-dimensional arrays, the front-end IC, and flip-chip bonding are discussed.

II. CMUT ARRAY

In this paper, a summary of the CMUT array design and fabrication is given [4]. A more detailed discussion of the fabrication and characterization of these arrays is given in [5]. Two-dimensional arrays with both 150- μm elements and 250- μm elements were fabricated. For each type of array, elements with varying membrane diameters were fabricated. The total die size for the 150- μm element arrays is 2.4 mm by 2.9 mm. The 250- μm element arrays are 4 mm by 4.7 mm. The arrays are slightly larger in one direction due to a row of pads used to connect to the CMUT DC bias voltage. Pictures of an array with 16 \times 16 250- μm elements are shown in Figure 2. A summary of the key process parameters is given in Table 1.

To characterize the uniformity of the arrays, for each of the 256 elements, the resonant frequency in air and input capacitance were measured. For the fully characterized array, the mean resonant frequency is 13.4 MHz with a standard deviation of 70 kHz. The mean device capacitance including the through-wafer interconnect is 1.3 pF with a standard deviation of 90 fF. The through-wafer interconnects were independently characterized. They have a mean capacitance of 60 fF, which is a significant reduction in capacitance compared with our group's previous results. The interconnect capacitance combined with the capacitance of the flip-chip bond pad is approximately 0.2 pF.

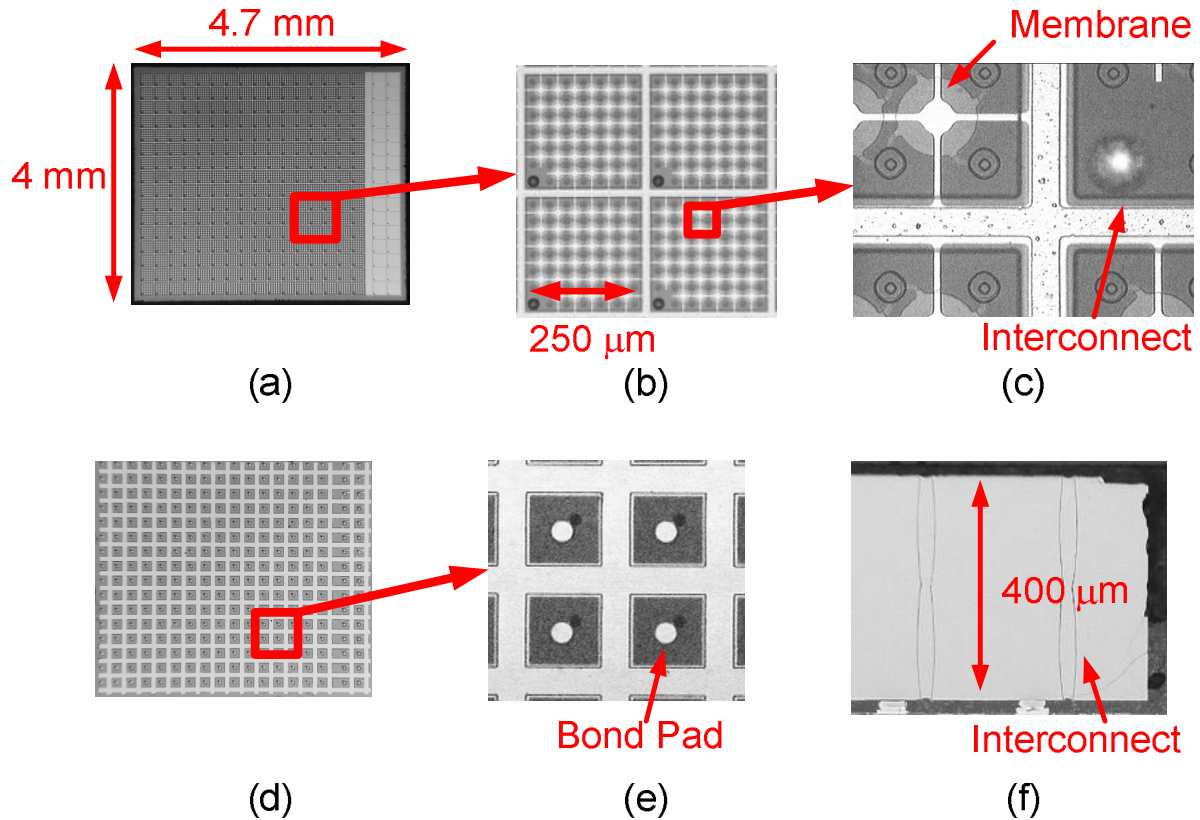


Figure 2: (a) The front side of the array. (b) A close-up of four elements. Each element consists of many membranes. (c) A close-up showing a membrane and the top side of the through-wafer interconnect. (d) The back side of the array. (e) The back side showing the flip-chip bond pads and opposite side of through-wafer interconnects. (f) A cross section illustrating the through-wafer interconnect.

Table 1: Key process parameters.

Cell diameter, μm	24, 30, 36
Element pitch, μm	150, 250
Number of cells per element	24, 35, 48
Membrane thickness, μm	0.6, 0.8
Cavity thickness, μm	0.05–0.15
Insulating layer thickness, μm	0.15
Silicon substrate thickness, μm	400
Flip-chip bond pad diameter, μm	50
Through-wafer interconnect diameter, μm	20
Silicon wafer resistivity, $\Omega\text{-cm}$	> 10,000

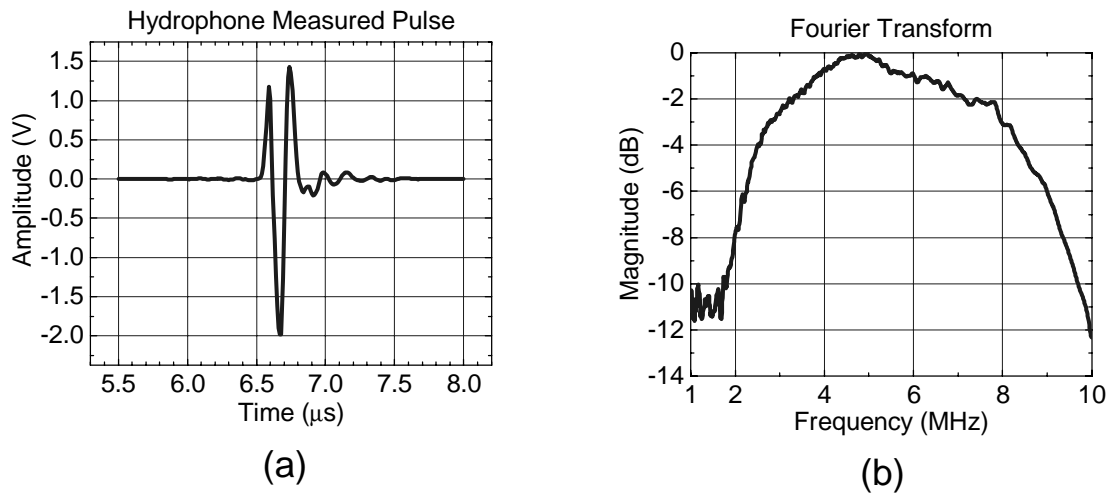


Figure 3: Pitch-catch hydrophone measurements. (a) Received pulse. (b) Fourier transform of received pulse.

Pitch-catch measurements were made with a hydrophone. The results are shown in Figure 3. For a 30-V, 100-ns wide pulse, the measured far-field pressure extrapolated to the face is 100 kPa.

III. FRONT-END INTEGRATED CIRCUIT

Integrating the front-end electronics with the transducer array mitigates the effects of the cables connecting the transducer probe with an external system. For imaging with an endoscope or catheter, the connecting cables can be several meters in length, introducing significant parasitic capacitance. Furthermore, signals received from the transducer are weak and subject to RF interference. An amplifier placed next to the transducer amplifies the received signals and can drive the parasitic capacitance of the cables. With additional circuitry, multiple receive channels could be multiplexed on a single cable reducing the number of cables required to connect to an external system.

In this implementation of the front-end IC, each of the 256 transducer elements is connected to a dedicated amplifier and pulser. The amplifier, pulser, transmit/receive switch combination is termed a unit cell. A schematic of the unit cell is shown in Figure 4(a). A sample transmit/receive sequence is shown in Figure 4(b).

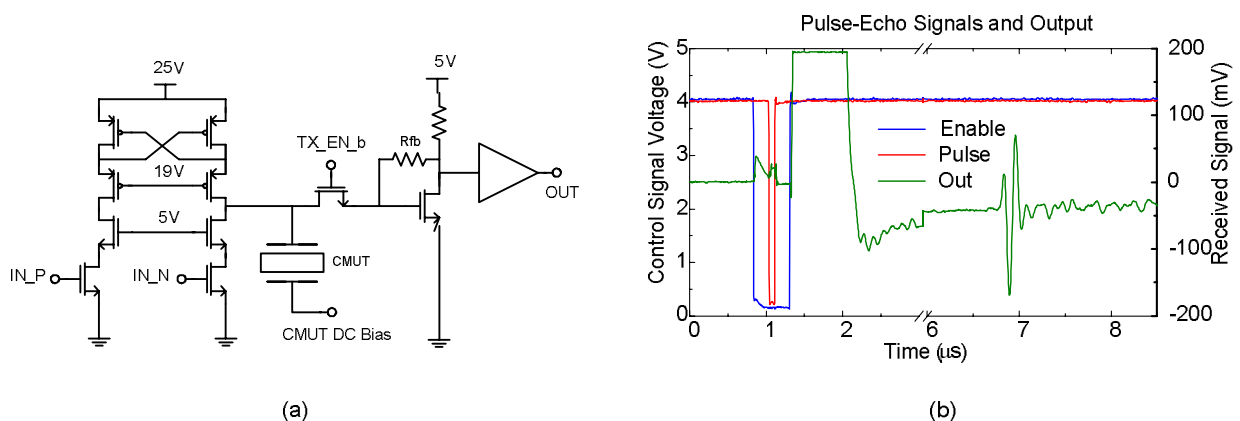


Figure 4: (a) The pulser, amplifier, and transmit/receive switch form the unit cell. (b) Pulse-echo signals and output.

Each unit cell contains: a pulser that generates 25-V, 100-ns wide, unipolar pulses; a switch that protects the low-voltage amplifier circuitry from the high-voltage pulse; and a low-noise transimpedance amplifier with a 500-k Ω transimpedance gain and 10-MHz bandwidth. To transmit, TX_EN_b is set low to open the switch. TX_PULSE

dictates the timing and duration of the pulse. When TX_EN_b goes high, signals IN_P and IN_N are set low and the pulser enters a high impedance state, the switch closes, and the amplifier is switched on to amplify the received signals.

In the initial implementation, only a single unit cell is active at a time. An individual cell is selected with 4-bit row and column addresses. Since only a single cell is active at a time, all of the outputs for a given column are connected together and share a common output buffer. The outputs of the 16 output buffers, corresponding to the 16 columns, are tied together and share a single output pin.

Each unit cell occupies an area of 250 μm by 250 μm and contains the circuitry shown in Figure 4(a). The row and column decoders, output buffers, and pads surround the unit cell array. The entire chip is 5.6 mm by 6.9 mm. The unit cell array occupies an area of 4 mm by 4 mm. A substantial part of the area beyond the unit cell array area is provided to ensure the flip-chip bonding process doesn't interfere with the bond pads on the periphery of the circuit. As we gain more experience with flip-chip bonding, we expect to reduce this excess area.

The CMUT equivalent circuit model is helpful in the design and analysis of the pulser and preamplifier [5,6]. The equivalent circuit model, derived from Mason's transducer model, is shown in Figure 6(a). Further simplified versions are shown in Figure 6(b) and Figure 6(c).

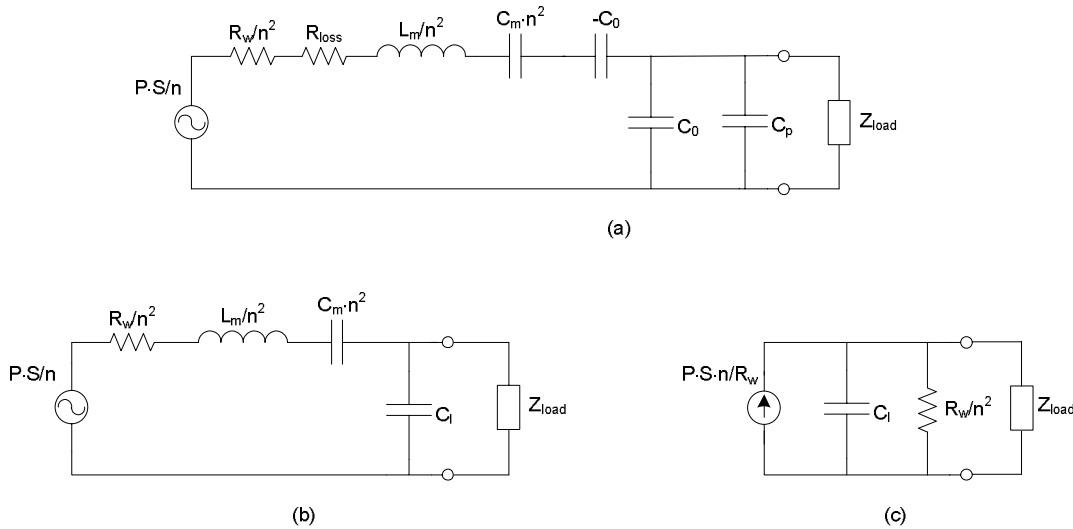


Figure 6: (a) The CMUT equivalent circuit. (b) The simplified circuit referred to the electrical port. (c) A further simplified version.

The component values in the circuit and their units are defined as follows.

$P \equiv$ Pressure (Pa)

$S \equiv$ Area of transducer (m^2)

$R_w = R_{med} \cdot S \equiv$ Medium resistance ($\text{Rayl} \cdot \text{m}^2$)

$R_{loss} \equiv$ Mechanical membrane loss ($\text{Pa} \cdot \text{m} \cdot \text{s}$)

$L_m, C_m \equiv$ Mechanical membrane impedance ($\text{Pa} \cdot \text{m}, \text{Pa}^{-1} \cdot \text{m}^{-1} \cdot \text{s}^{-2}$)

$n \equiv$ Transformer ratio (N/V)

$C_0 \equiv$ Device capacitance (pF)

$Z_{load} \equiv$ Amplifier load impedance (Ω)

$C_1 \equiv C_0 + C_p$

The membrane impedance, transformer ratio, and device capacitance are obtained from a simulation tool developed in our group.

A summary of the IC performance is given in Table 2. A photo of the circuit is shown in Figure 9.

Table 2: Circuit performance summary.

Total power	8.5 mW (6 μ W when no element is selected)
Supply voltages	5 V, 25 V
Amplifier DC transimpedance gain	510 k Ω
Approximate amplifier bandwidth	10 MHz
Amplifier startup time	900 nS
Approximate minimum pulse width	100 ns
Maximum pulse voltage	25 V

IV. FLIP-CHIP BONDING

For the results presented here, Promex Industries, Santa Clara, CA performed the flip-chip bonding. The process used by Promex is based on anisotropic conducting film (ACF). In this process, gold bumps are first applied to the IC using a standard wire bonder. The ACF is placed between the CMUT and IC and the two parts are aligned and pressed together. The ACF only conducts where it is squeezed between the gold bumps and the CMUT, thus providing the connections between the IC and CMUT array. Figures 10(a) and 10(b) illustrate this process. The IC covered with gold bumps is shown in Figure 10(a). Figure 10(b) shows a cross-sectional view of the bonded IC and CMUT. The packaged and flip-chip bonded IC and CMUT array are shown in Figure 11. Our group is also developing a flip-chip bonding process which is described in [5].

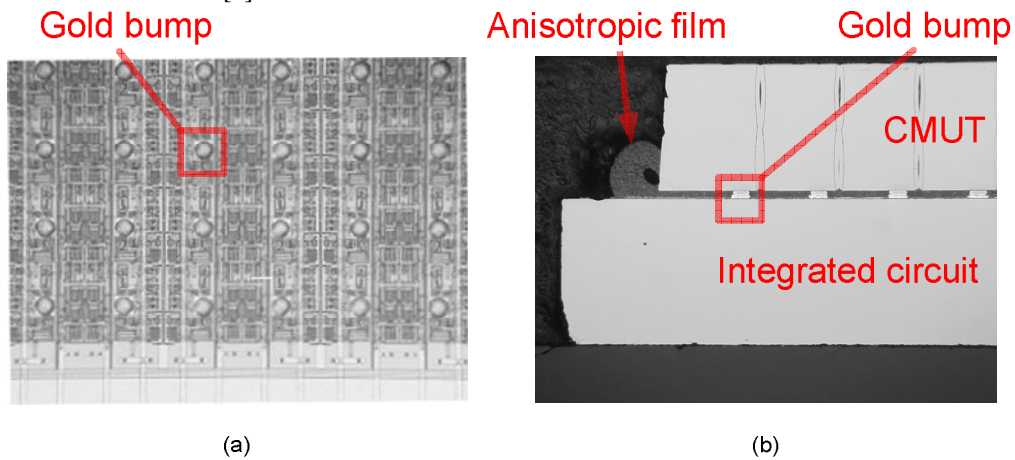


Figure 10: (a) Gold bumps applied to front-end IC. (b) Cross-section of flip-chip bonded IC and CMUT array.

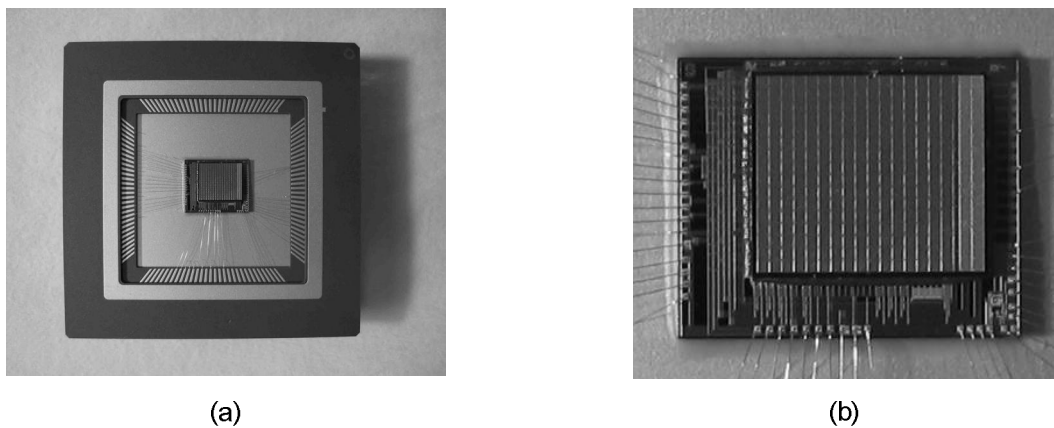


Figure 11: (a) Packaged CMUT array flip-chip bonded to IC. (b) Close-up view of bonded CMUT and IC.

The first effort using the ACF-based process had poor yield. Only 40 of the 256 elements showed connectivity between the CMUT and IC. The poor yield is due to misalignment between the IC and CMUT. This misalignment is illustrated by the cross-sectional views shown in Figure 12. In Figure 12(a), the bond pad on the CMUT side is severely misaligned with respect to the gold bump and thus there is no connection between the CMUT and IC. However, in Figure 12(b), there is some overlap between the pad and gold bump providing connectivity.

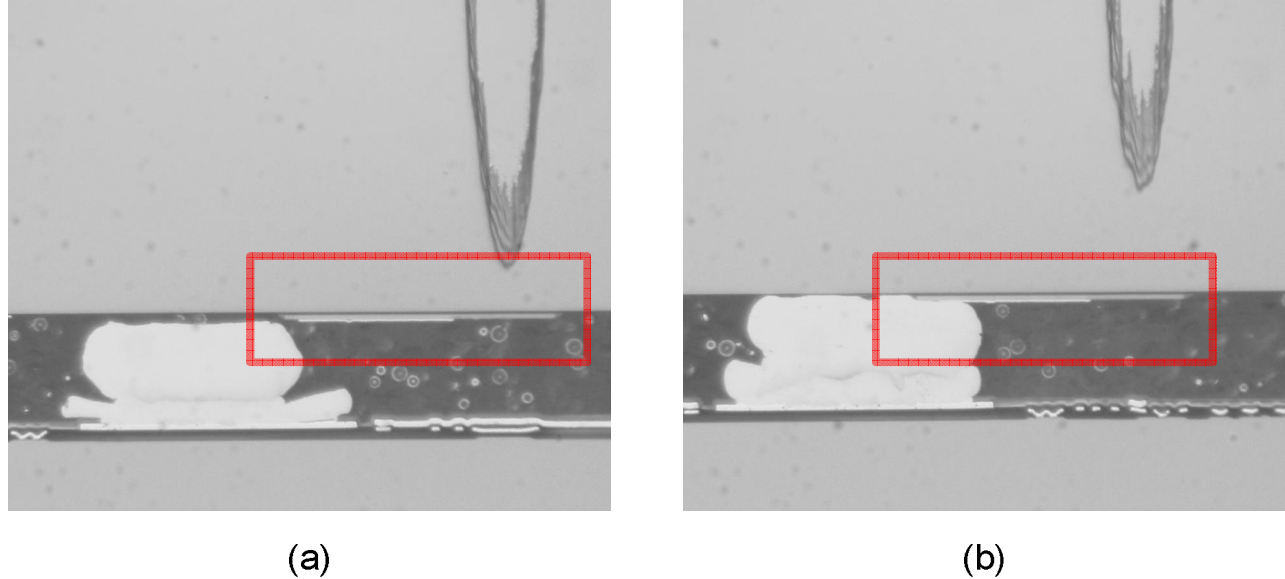


Figure 12: (a) Misaligned CMUT and IC pads with no connection. (b) Overlapping CMUT and IC pads.

Flip-chip bonding is a mature technology used in industry to reliably make large numbers of connections. Thus, we are confident with more work on our own process and collaboration with packaging companies, 100% flip-chip bond yield will be achieved.

V. PULSE-ECHO RESULTS

The flip-chip bonded IC and CMUT array were submerged in oil and pulse-echo measurements were made. The reflection from the air-oil interface at 5 mm is shown in Figure 13(a). The Fourier transform of the pulse is shown in Figure 13(b).

The center frequency of the pulse is at approximately 7 MHz. The array for which 40 of the flip-chip bond connections are good has smaller membranes than the array intended for 5-MHz operation. This explains the slightly higher center frequency. The bandwidth of the echo signal is 85%. In Figure 13(a), some ringing can be seen following the pulse. This ringing is at approximately 10 MHz which is also consistent with the dip seen in the Fourier transform. This ringing is due to substrate reflections. In this case, this interference occurs outside the intended 2.5-7.5-MHz bandwidth and thus can be filtered out. If the frequency of this ringing falls within the intended band, the frequency at which the substrate ringing occurs can be moved by modifying the thickness of the substrate. The peak-to-peak pressure of the transmitted pulse was measured with a hydrophone. The pressure normalized to the face of the transducer is 75 kPa.

Figure 14 illustrates the variation in transducer performance seen over the 40 elements that are connected to the IC.

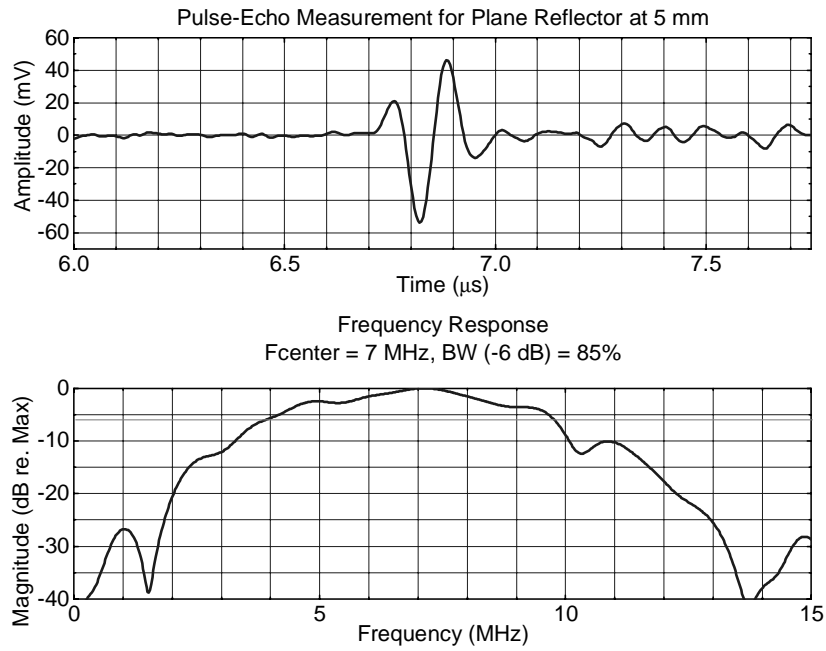


Figure 13: (a) Pulse received from plane reflector at 5 mm. (b) Fourier transform of pulse-echo pulse.

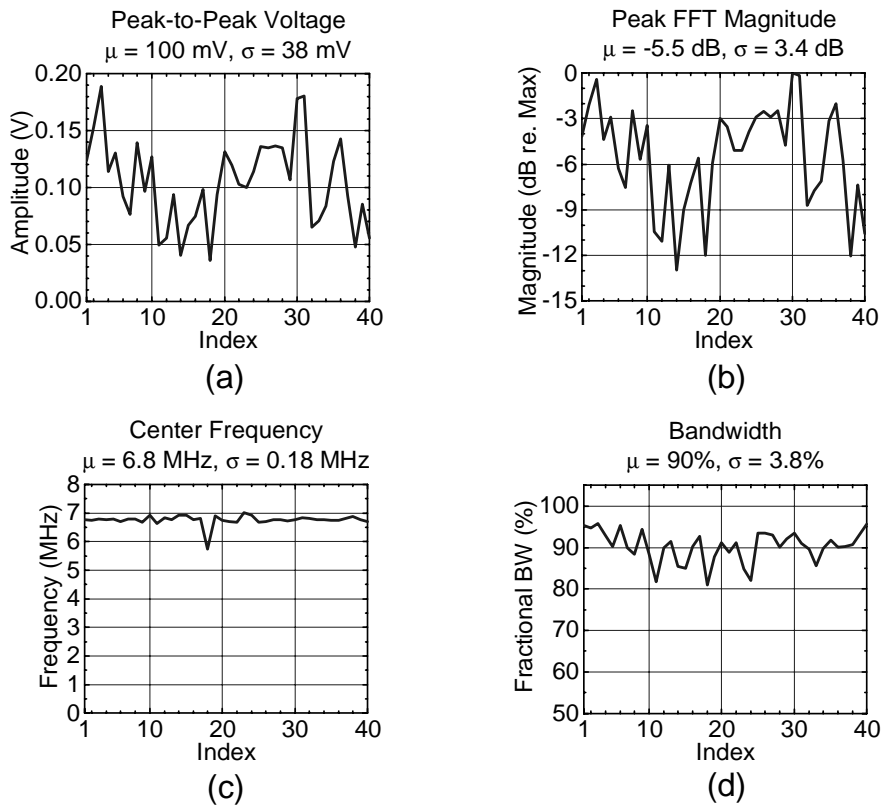


Figure 14: Variation across 40 connected elements.

Figures 14(a) and 14(b) show the variation in received amplitude over the 40 connections. Figure 14(a) gives the variation in peak-to-peak voltage of the pulse-echo signal. Figure 14(b) shows the variation in the amplitude of the Fourier transform at the center frequency. Figure 14(c) shows the variation in center frequency and Figure 14(d) shows the variation in fractional bandwidth. Because the flip-chip bonding connections are so sporadic, it's difficult to isolate the sources of the variations illustrated in Figure 14. Much of the variation may be due to poor connections between the IC and CMUT array. With better bonding we expect to see more uniform performance.

V. CONCLUSION

The imaging system described in this paper demonstrates the advantages of the CMUT technology. The fabrication flexibility of silicon micromachining means that fully populated two-dimensional arrays, small enough to fit inside an endoscope channel, can be reliably fabricated. Bulk silicon micromachining enables the creation of through-wafer interconnects, which allow the CMUT array to be compactly connected to a front-end integrated circuit for improved SNR. In this paper, results from the front-end IC, CMUT arrays, and flip-chip bonding are discussed. These results demonstrate the feasibility of integrating the front-end electronics with the transducer array. With further development of the flip-chip bonding process, we will be ready to incorporate the transducer array and integrated electronics into a data acquisition and image reconstruction system.

ACKNOWLEDGMENTS

We would like to thank Omair Saadat for his work on the PCB and data acquisition system design. We would like to thank National Semiconductor for fabrication of the circuits described in this paper. Specifically, Bill Broach and the members of the Portable Power Group at National Semiconductor provided valuable circuit and process information. The National Institutes of Health funded this work. Xuefeng Zhuang is supported by a Weiland Family Stanford Graduate Fellowship. David Yeh is supported by a National Defense Science and Engineering Graduate Fellowship.

REFERENCES

- [1] C. H. Cheng, E. M. Chow, X. Jin, A. S. Ergun, and B. T. Khuri-Yakub, "An efficient electrical addressing method using through-wafer vias for two-dimensional ultrasonic arrays," in Proc. IEEE Ultrason. Symp., 2000, pp. 1179 – 1182.
- [2] C. H. Cheng, A. S. Ergun, and B. T. Khuri-Yakub, "Electrical through-wafer interconnects with sub-picofarad parasitic capacitance," in Microelectromechanical Systems Conference, 2001, pp. 18 – 21.
- [3] C. H. Cheng, A. S. Ergun, and B. T. Khuri-Yakub, "Electrical through-wafer interconnects with 0.05 pico farads parasitic capacitance on 400 μm thick silicon substrates", in Solid-State Sensor and Actuator Work-shop, 2002, pp. 157-160.
- [4] A. S. Ergun, C. H. Cheng, U. Demirci, and B. T. Khuri-Yakub, "Fabrication and characterization of 1-dimensional and 2-dimensional capacitive micromachined ultrasonic transducer (CMUT) arrays for 2 dimensional and volumetric ultrasonic imaging," in MTS/IEEE Oceans, 2002, pp. 2361 – 2367.
- [5] X. Zhuang, I. O. Wygant, D. T. Yeh, A. Nikoozadeh, O. Oralkan, A. S. Ergun, C-H. Cheng, Y. Huang, G. G. Yaralioglu, and B. T. Khuri-Yakub, "Two-Dimensional Capacitive Micromachined Ultrasonic Transducer (CMUT) Arrays for a Miniature Integrated Volumetric Ultrasonic Imaging System," presented at SPIE Medical Imaging Conference, San Diego, CA, Feb. 12-17, 2005.
- [6] W. P. Mason, *Electromechanical Transducers and Wave Filters*. London: Van Nostrand, 1948.
- [7] G. G. Yaralioglu, M. H. Badi, A. S. Ergun and B. T. Khuri-Yakub, "Improved equivalent circuit and finite element method modeling of capacitive micromachined ultrasonic transducers," in Proc. IEEE Ultrason. Symp., 2003, pp. 469-472.
- [8] J. Graeme, *Photodiode Amplifiers: Op Amp Solutions*, McGraw-Hill, Boston, 1996.